



Oxidation of silicon nanowire can transport much more light into silicon substrate

YINGFENG LI, WENJIAN LIU, YOUNAN LUO, MENGQI CUI, AND MEICHENG LI*

State Key Laboratory of Alternate Electrical Power System with Renewable Energy Sources, North China Electric Power University, Beijing, 102206, China

*mcli@ncepu.edu.cn

Abstract: Silicon nanowire (SiNW) has been widely used for light-trapping in photovoltaics, optical sensors, and other optoelectronic devices. However, we found that 58.4% of the light trapped by a SiNW with a diameter of 60 nm and a length of 1 μm will be wasted: 64.5% of the trapped light will be absorbed within itself, and 90.5% of carriers excited by this part of light will recombine before being transported to the silicon substrate. In this work, it is shown that oxidation of SiNW can transport much more light into the silicon substrate. At first, our simulation results demonstrate that oxidation can dramatically reduce the percentage of absorbed light. In an oxidized SiNW (O-SiNW) with a total and silicon core diameter of 60 nm and 30 nm, respectively, the percentage is about 44.5%. Next, a low carrier recombination ratio, about 27.3%, can be obtained in O-SiNW due to the passivation effect of the oxide layer. As a result, oxidation of SiNW can reduce the proportion of wasted light from 58.4% to 12.1%. More importantly, oxidation almost doesn't sacrifice the light-trapping ability: experimental measurements demonstrate that the average reflectance of an O-SiNW array is only slightly higher than that of a SiNW array, 3.9% vs. 3.0%. Such O-SiNW is promising to be used for low-loss light-trapping in specially designed photovoltaic devices.

© 2017 Optical Society of America under the terms of the [OSA Open Access Publishing Agreement](#)

OCIS codes: (350.6050) Solar energy; (000.4430) Numerical approximation and analysis; (160.4760) Optical properties; (160.4236) Nanomaterials.

References and links

1. E. Garnett and P. Yang, "Light trapping in silicon nanowire solar cells," *Nano Lett.* **10**(3), 1082–1087 (2010).
2. B. Tian, X. Zheng, T. J. Kempa, Y. Fang, N. Yu, G. Yu, J. Huang, and C. M. Lieber, "Coaxial silicon nanowires as solar cells and nanoelectronic power sources," *Nature* **449**(7164), 885–889 (2007).
3. Y. Li, M. Li, D. Song, H. Liu, B. Jiang, F. Bai, and L. Chu, "Broadband light-concentration with near-surface distribution by silver capped silicon nanowire for high-performance solar cells," *Nano Energy* **11**, 756–764 (2015).
4. H. Park, Y. Dan, K. Seo, Y. J. Yu, P. K. Duane, M. Wober, and K. B. Crozier, "Filter-free image sensor pixels comprising silicon nanowires with selective color absorption," *Nano Lett.* **14**(4), 1804–1809 (2014).
5. F. M. Zörgiebel, S. Pregl, L. Römhildt, J. Opitz, W. Weber, T. Mikolajick, L. Baraban, and G. Cuniberti, "Schottky barrier-based silicon nanowire pH sensor with live sensitivity control," *Nano Res.* **7**, 263–271 (2014).
6. S. Chen, A. van den Berg, and E. T. Carlen, "Sensitivity and detection limit analysis of silicon nanowire bio (chemical) sensors," *Sens. Actuators B Chem.* **209**, 486–489 (2015).
7. L. Cao, J.-S. Park, P. Fan, B. Clemens, and M. L. Brongersma, "Resonant germanium nanoantenna photodetectors," *Nano Lett.* **10**(4), 1229–1233 (2010).
8. P. Fan, U. K. Chettiar, L. Cao, F. Afshinmanesh, N. Engheta, and M. L. Brongersma, "An invisible metal-semiconductor photodetector," *Nat. Photonics* **6**, 380–385 (2012).
9. H. Park and K. B. Crozier, "Elliptical silicon nanowire photodetectors for polarization-resolved imaging," *Opt. Express* **23**(6), 7209–7216 (2015).
10. R. H. Coridan, K. A. Arpin, B. S. Brunschwig, P. V. Braun, and N. S. Lewis, "Photoelectrochemical Behavior of Hierarchically Structured Si/WO₃ Core-Shell Tandem Photoanodes," *Nano Lett.* **14**(5), 2310–2317 (2014).
11. H. Han, Z. Huang, and W. Lee, "Metal-assisted chemical etching of silicon and nanotechnology applications," *Nano Today* **9**, 271–304 (2014).
12. M. C. McAlpine, H. Ahmad, D. Wang, and J. R. Heath, "Highly ordered nanowire arrays on plastic substrates for ultrasensitive flexible chemical sensors," *Nat. Mater.* **6**(5), 379–384 (2007).
13. K.-Q. Peng, X. Wang, L. Li, Y. Hu, and S.-T. Lee, "Silicon nanowires for advanced energy conversion and storage," *Nano Today* **8**, 75–97 (2013).
14. M. D. Kelzenberg, S. W. Boettcher, J. A. Petykiewicz, D. B. Turner-Evans, M. C. Putnam, E. L. Warren, J. M. Spurgeon, R. M. Briggs, N. S. Lewis, and H. A. Atwater, "Enhanced absorption and carrier collection in Si wire

- arrays for photovoltaic applications,” *Nat. Mater.* **9**(3), 239–244 (2010).
15. P. Krogstrup, H. I. Jørgensen, M. Heiss, O. Demichel, J. V. Holm, M. Aagesen, J. Nygard, and A. F. I. Morral, “Single-nanowire solar cells beyond the Shockley-Queisser limit,” *Nat. Photonics* **7**, 306–310 (2013).
 16. E. Garnett and P. Yang, “Light Trapping in Silicon Nanowire Solar Cells,” *Nano Lett.* **10**(3), 1082–1087 (2010).
 17. Y. Li, M. Li, R. Li, P. Fu, T. Wang, Y. Luo, J. M. Mbengue, and M. Trevor, “Exact comprehensive equations for the photon management properties of silicon nanowire,” *Sci. Rep.* **6**, 24847 (2016).
 18. Y. Li, L. Yue, Y. Luo, W. Liu, and M. Li, “Light harvesting of silicon nanostructure for solar cells application,” *Opt. Express* **24**(14), A1075–A1082 (2016).
 19. Y.-J. Lee, Y.-C. Yao, and C.-H. Yang, “Direct electrical contact of slanted ITO film on axial p-n junction silicon nanowire solar cells,” *Opt. Express* **21**(Suppl 1), A7–A14 (2013).
 20. A. Smyrnakis, P. Dimitrakakis, P. Normand, and E. Gogolides, “Fabrication of axial p-n junction silicon nanopillar devices and application in photovoltaics,” *Microelectron. Eng.* **174**, 74–79 (2017).
 21. S. Perraud, S. Poncet, S. Noël, M. Levis, P. Faucherand, E. Rouvière, P. Thony, C. Jaussaud, and R. Delsol, “Full process for integrating silicon nanowire arrays into solar cells,” *Sol. Energy Mater. Sol. Cells* **93**, 1568–1571 (2009).
 22. D. Kanematsu, S. Yata, A. Terakawa, M. Tanaka, and M. Konagai, “Photovoltaic properties of axial-junction silicon nanowire solar cells with integrated arrays,” *Jpn. J. Appl. Phys.* **54**, 08KA09 (2015).
 23. T. J. Kempa, B. Tian, D. R. Kim, J. Hu, X. Zheng, and C. M. Lieber, “Single and tandem axial p-i-n nanowire photovoltaic devices,” *Nano Lett.* **8**(10), 3456–3460 (2008).
 24. Y. Li, M. Li, R. Li, P. Fu, L. Chu, and D. Song, “Method to determine the optimal silicon nanowire length for photovoltaic devices,” *Appl. Phys. Lett.* **106**, 091908 (2015).
 25. J. D. Christesen, X. Zhang, C. W. Pinion, T. A. Celano, C. J. Flynn, and J. F. Cahoon, “Design principles for photovoltaic devices based on Si nanowires with axial or radial p-n junctions,” *Nano Lett.* **12**(11), 6024–6029 (2012).
 26. M. D. Kelzenberg, D. B. Turner-Evans, B. M. Kayes, M. A. Filler, M. C. Putnam, N. S. Lewis, and H. A. Atwater, “Photovoltaic measurements in single-nanowire silicon solar cells,” *Nano Lett.* **8**(2), 710–714 (2008).
 27. J. K. Mann, R. Kurtstjens, G. Pourtois, M. Gilbert, F. Dross, and J. Poortmans, “Opportunities in nanometer sized Si wires for PV applications,” *Prog. Mater. Sci.* **58**, 1361–1387 (2013).
 28. A. B. Sieval, C. L. Huisman, A. Schönecker, F. M. Schuurmans, A. S. van der Heide, A. Goossens, W. C. Sinke, H. Zuilhof, and E. J. Sudhölter, “Silicon surface passivation by organic monolayers: minority charge carrier lifetime measurements and Kelvin probe investigations,” *J. Phys. Chem. B* **107**, 6846–6852 (2003).
 29. J. Oh, H.-C. Yuan, and H. M. Branz, “An 18.2%-efficient black-silicon solar cell achieved through control of carrier recombination in nanostructures,” *Nat. Nanotechnol.* **7**(11), 743–748 (2012).
 30. Y. Li, Y. Luo, W. Liu, M. Cui, J. Kumar, B. Jiang, L. Chu, and M. Li, “Specific distribution of the light captured by silver nanowire,” *Opt. Express* **25**(8), 9225–9231 (2017).
 31. B. T. Draine and P. J. Flatau, “User guide for the discrete dipole approximation code DDSCAT 7.3,” arXiv:1305.6497 (2013).
 32. J. E. Allen, E. R. Hemesath, D. E. Perea, J. L. Lensch-Falk, Z. Y. Li, F. Yin, M. H. Gass, P. Wang, A. L. Bleloch, R. E. Palmer, and L. J. Lauhon, “High-resolution detection of Au catalyst atoms in Si nanowires,” *Nat. Nanotechnol.* **3**(3), 168–173 (2008).
 33. Y. Dan, K. Seo, K. Takei, J. H. Meza, A. Javey, and K. B. Crozier, “Dramatic reduction of surface recombination by in situ surface passivation of silicon nanowires,” *Nano Lett.* **11**(6), 2527–2532 (2011).
 34. M. Y. Bashouti, K. Sardashti, S. W. Schmitt, M. Pietsch, J. Ristein, H. Haick, and S. H. Christiansen, “Oxide-free hybrid silicon nanowires: From fundamentals to applied nanotechnology,” *Prog. Surf. Sci.* **88**, 39–60 (2013).
 35. Y. Cui, Z. Zhong, D. Wang, W. U. Wang, and C. M. Lieber, “High performance silicon nanowire field effect transistors,” *Nano Lett.* **3**, 149–152 (2003).
 36. S. Kato, Y. Kurokawa, S. Miyajima, Y. Watanabe, A. Yamada, Y. Ohta, Y. Niwa, and M. Hirota, “Improvement of carrier diffusion length in silicon nanowire arrays using atomic layer deposition,” *Nanoscale Res. Lett.* **8**(1), 361 (2013).
 37. Y. Li, P. Fu, R. Li, M. Li, Y. Luo, and D. Song, “Ultrathin flexible planar crystalline-silicon/polymer hybrid solar cell with 5.68% efficiency by effective passivation,” *Appl. Surf. Sci.* **366**, 494–498 (2016).
 38. P. Werner, C. C. Büttner, L. Schubert, G. Gerth, N. D. Zakarov, and U. Gösele, “Gold-enhanced oxidation of silicon nanowires,” *Int. J. Mater. Res.* **98**, 1066–1070 (2007).
 39. V. A. Sivakov, R. Scholz, F. Syrowatka, F. Falk, U. Gösele, and S. H. Christiansen, “Silicon nanowire oxidation: the influence of sidewall structure and gold distribution,” *Nanotechnology* **20**(40), 405607 (2009).
 40. J. Kioseoglou, P. Komninou, and M. Zervos, “Thermal oxidation and facet formation mechanisms of Si nanowires,” *Phys. Status Solidi* **8**, 307–311 (2014).
 41. S. Krylyuk, A. V. Davydov, I. Levin, A. Motayed, and M. D. Vaudin, “Rapid thermal oxidation of silicon nanowires,” *Appl. Phys. Lett.* **94**, 063113 (2009).
 42. U. Khalilov, G. Pourtois, A. v. Duin, and E. Neyts, “Self-limiting oxidation in small-diameter Si nanowires,” *Chem. Mater.* **24**, 2141–2147 (2012).
 43. M. Karylaoui, A. Bardaoui, M. B. Rabha, J. Harmand, and M. Amlouk, “Effect of rapid oxidation on optical and electrical properties of silicon nanowires obtained by chemical etching,” *Eur. Phys. J. Appl. Phys.* **58**, 20103 (2012).

44. T. Xie, V. Schmidt, E. Pippel, S. Senz, and U. Gösele, "Gold-Enhanced Low-Temperature Oxidation of Silicon Nanowires," *Small* **4**(1), 64–68 (2008).
45. C. Büttner, N. Zakharov, E. Pippel, U. Gösele, and P. Werner, "Gold-enhanced oxidation of MBE-grown silicon nanowires," *Semicond. Sci. Technol.* **23**, 075040 (2008).
46. S. Su, L. Lin, Z. Li, J. Feng, and Z. Zhang, "The fabrication of large-scale sub-10-nm core-shell silicon nanowire arrays," *Nanoscale Res. Lett.* **8**(1), 405 (2013).
47. S. Jeong, M. D. McGehee, and Y. Cui, "All-back-contact ultra-thin silicon nanocone solar cells with 13.7% power conversion efficiency," *Nat. Commun.* **4**, 2950 (2013).
48. H. F. Li, R. Jia, C. Chen, Z. Xing, W. C. Ding, Y. L. Meng, D. Q. Wu, X. Y. Liu, and T. C. Ye, "Influence of nanowires length on performance of crystalline silicon solar cell," *Appl. Phys. Lett.* **98**, 3574904 (2011).
49. E. C. Garnett and P. Yang, "Silicon nanowire radial p-n junction solar cells," *J. Am. Chem. Soc.* **130**(29), 9224–9225 (2008).

1. Introduction

Recently, silicon nanowire (SiNW) has attracted extensive attention in solar cells [1–3], optical sensors [4–6], photon detectors [7–9], optical chemistry [10] and other optoelectronic devices [11–14]. An important reason is that SiNW shows extraordinary light-trapping ability, which has been verified theoretically and experimentally [14–18]. A single SiNW can harvest light in the area several tens of times more than its geometrical cross-section [13–15].

However, the reported performances of solar cells using SiNW as the light-trapping structure are far away from the expectation [19–23]: the maximum power conversion efficiency is only 4.1% [20]. Such a bad performance can be attributed to two aspects. The first one is that although SiNW has the excellent light-trapping ability, a great part of the trapped sunlight will be absorbed within itself [3,24]. Such absorbed light will excite charge carriers in situ, therefore, these carriers must go through the nanowire before being collected by the electrodes [25,26]. The second one is that the abundant surface defect sites on SiNW will cause serious carrier recombination [27–29]. The strong intrinsic light absorption collaborating with the serious carrier recombination during the axial transportation of carriers will result in strong sunlight loss, which seriously limits the performance of photovoltaic devices using SiNW as the light-trapping layer [20] or the ones with axial PN junction structure on the nanowire [25]. So, it is of great significance to reduce the intrinsic light absorption and/or carrier recombination in SiNW.

In this study, we show that oxidation of SiNW can reduce both of the intrinsic light absorption and the carrier recombination in SiNW, i.e., transport more light into the silicon substrate. Based on discrete dipole approximation (DDA) simulations it is found that, in oxidized SiNW (O-SiNW), the proportion of light loss, 12.1%, is quite smaller than that in SiNW, 58.4%. At the same time, light reflectance measurements on several O-SiNW arrays demonstrate that oxidation almost doesn't sacrifice the light-trapping ability. This study provides an easy practical way to accomplish high-effective low-loss light-trapping. The O-SiNW can be used in specially designed devices like all-back-contact or selective-textured solar cells.

2. Simulations and experiments

2.1 Simulations

The amount of light concentrated by O-SiNW under the irradiation of unit-intensity light is defined as its extinction cross section, C_{ext} . Similarly, the amount of light being absorbed is defined as the absorption cross section, C_{abs} . Correspondingly, the extinction efficiency, Q_{ext} (the absorption efficiency, Q_{abs}), is defined as the ratio between C_{ext} (C_{abs}) and the projected area of SiNW along the light.

A schematic diagram which illustrates the light concentration effect of an O-SiNW is given in Fig. 1(a). As the incident angle used in measuring the reflectance spectrum of a nanowire array is usually between 0 and 5°; and in this range, the influence of incident angle on the light concentration effect of a nanowire is very weak [30], only the light irradiating from the top of O-SiNW is considering here. In this situation, Q_{ext} and Q_{abs} can be simply

described as $Q_{ext} = C_{ext}/\pi r^2$ and $Q_{abs} = C_{abs}/\pi r^2$, where r is the radius of the nanowire. These two physical quantities denote the light-concentration and light-absorption abilities (multiples) of SiNW, respectively.

The extinction and absorption efficiencies, Q_{ext} and Q_{abs} , were simulated using the DDA method by DDSCAT 7.3 [31]. In all simulations, the interdipole separation, d , was set as 3.3 nm; the error tolerance, h , was set to be 1×10^{-5} . Descriptions of the physical foundation and framework of the DDA method can be found elsewhere [3].

2.2 Experiments

The SiNW was fabricated by the metal-assisted chemical etching on *n*-type Si (100) wafer. In the first step, the silicon wafer was systematically cleaned: *i*) it was ultrasonically cleaned in acetone, ethanol, and ultrapure water for 10 minutes respectively; *ii*) the cleaned sample was rinsed with deionized water for several times; *iii*) the rinsed sample was immersed in hydrofluoric acid (HF) to eliminate the native oxide layer and to reduce the surface defect by forming Si-H bonds; *iv*), the sample was washed with deionized water and dried with high purity nitrogen repeatedly. Then, the cleaned silicon wafer was placed into the ultraviolet ozone washing machine to modify the surface, which is helpful for a uniform etching. Next, the surface-modified silicon wafer was immersed in a mixed solution of 0.02 M AgNO₃, 4.6 M HF and deionized water for 3 min at room temperature to fabricate SiNW. In this process, the size and morphology of SiNW can be adjusted by the temperature and the etching time. Finally, the SiNW were immersed into the concentrated HNO₃ solution to remove the residual silver complex; and after that the samples were cleaned using 7.5 M HF solution for 3 min to remove the oxide layer formed due to the oxidation of the concentrated HNO₃.

The O-SiNW was fabricated by the thermal oxidation method. The silicon wafer with SiNWs of diameter ~60 nm and length ~1 μm was put into a thermal chemical vapor deposition (CVD) tube furnace. The oxidation of SiNW was carried out at 1050 °C under an oxygen atmosphere, where the thickness of the oxidized layer (silica shell) was controlled by adjusting the oxidation time from 5 mins to 30 mins.

The morphologies of SiNW and O-SiNW were characterized using the Scanning Electron Microscopy (SEM; FEI Quanta 200F) and the Transmission Electron Microscopy (TEM; FEI Tecnai G2 F20). And an element mapping for O-SiNW was carried out using an Energy Dispersive X-ray Spectrometer (EDX) integrated in TEM. The reflectance spectrums of SiNW and O-SiNW arrays were measured using a Ultraviolet-Visible Spectrophotometer (UV-2006/2007; SHIMADZU).

3. Results and discussion

3.1 Light loss in SiNW

As the photons intrinsically absorbed within a SiNW can excite e-h pairs in situ, these carriers must experience long-distance transport thus abundant recombination before reaching the silicon substrate in SiNW-based solar cells. This means the amount of light absorbed by a SiNW will suffer from large loss; therefore, the proportion of absorbed light by SiNW was first investigated.

The extinction and absorption efficiency curves of a SiNW with a diameter of 60 nm and a length of 1 μm are given in Fig. 1(b). At first, it can be obviously seen that the maximum light-concentration multiple of SiNW (at the resonant wavelength) exceeds 100, which confirms the super light-concentration ability of SiNW as being reported [13–15]. The concentrated light can be separated into two parts: one part will be scattered forward into a cone of opening angle smaller than 30°, as denoted in Fig. 1(a) [3]; and the other part will be intrinsically absorbed within the SiNW itself. The fact should be noted is that the absorption efficiency of SiNW reaches 60 at the resonant wavelength. This denotes that a great ratio of the concentrated light will be intrinsically absorbed. Because SiNW is widely used to trap

sunlight, for more objective, a full-spectrum average Abs./Ext. is evaluated by $\int_{0.3}^{0.6} [Q_{abs}(\lambda)/Q_{ext}(\lambda)]I(\lambda)d\lambda / \int_{0.3}^{0.6} I(\lambda)d\lambda$, where λ is the wavelength and $I(\lambda)$ is the wavelength selective intensity of AM1.5. The calculated value, 64.5%, means 64.5% of sunlight concentrated by a SiNW will be absorbed within itself.

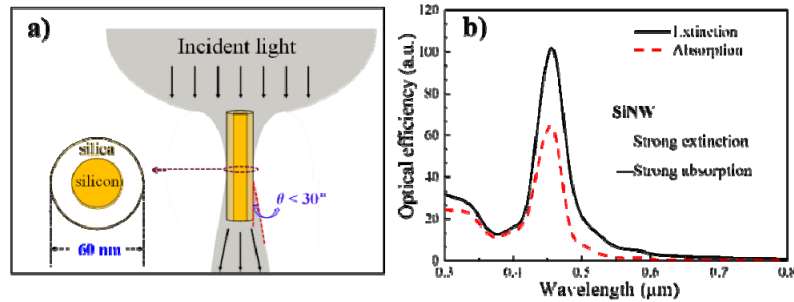


Fig. 1. (a) A schematic diagram of the light concentration effect of an O-SiNW; and (b) the extinction and absorption efficiency curves for a single SiNW with a diameter of 60 nm and a length of 1 μm .

The absorbed light within SiNW will be transferred to carriers in situ, which then transport along the nanowire till reach the silicon substrate. Next, the proportion of carriers being recombined during this transport process is evaluated, based on some reported data [32]. It is well known that according to the carrier transport equation, $1/e^{x/l}$ of the carriers can be left after transporting a distance of x , where l is the diffusion length of the carrier. If we assume that the light intensity is axial uniform in the SiNW [24], the equation for calculating the proportion of recombined carriers in a SiNW can be written to be $1 - \int_0^L 1/e^{x/l} dx$, where L is the length of SiNW. It has been reported that the carrier diffusion length in SiNW is even shorter than 100 nm [32]; therefore, in a SiNW of length 1 μm , the proportion of recombined carriers can be evaluated to be $1 - \int_0^{1000} 1/e^{x/100} dx = 90.5\%$. Comprehensively, there is $64.5\% \times 90.5\% \approx 58.4\%$ of the sunlight will be wasted when using SiNW as a light-trapping structure.

3.2 Oxidation of SiNW can significantly reduce light loss

According to above analyses, there may be two strategies to reduce the light loss: to reduce the the proportion of the absorbed light and to reduce the surface recombination rate. Surface passivation is a quite common method to reduce the surface recombination loss. Many surface passivations like $\alpha\text{-Si:H}$, Si-C, and Si-N passivations have been developed for SiNW, which can dramatically lengthen the diffusion length of the carrier [33–36]. However, as these techniques only modified the chemical properties of the SiNW surface, they have no effect on the optical features of SiNW at all. Therefore, these techniques can't be used to reduce the percentage of absorbed light for SiNW. Oxidation is also an effective passivate method for silicon surface [37]. By a so-called thermal oxidation technique, not only the surface of SiNW can be modified, but also an oxide layer with controllable thickness can be formed surrounding the SiNW [38–40]. The oxide layer provides a new dielectric circumstance for the silicon core, thus may provide an opportunity to reduce the proportion of the absorbed light.

The optical features of several O-SiNWs with a constant length of 1 μm , a constant total diameter of 60 nm, but various silicon core diameters from 10 nm to 50 nm are simulated. Figure 2(a) gives the wavelength selective extinction efficiency curves of various O-SiNWs which are denoted by 60@core-diameter. For each O-SiNW, the ratio between the absorbed

AMI.5 sunlight and the whole amount of sunlight it can concentrate, $Abs./Ext.$, can be also calculated by $\int_{0.3}^{0.6} [Q_{abs}(\lambda)/Q_{ext}(\lambda)]I(\lambda)d\lambda / \int_{0.3}^{0.6} I(\lambda)d\lambda$. The obtained results are plotted in Fig. 2(b) by a black line and red triangles. It can be seen that the ratio of absorbed light in O-SiNW decreases gradually from 64.5% to 5.2%, with the core diameter decreases from 60 nm to 10 nm. This demonstrates that the formation of a thick oxide layer surrounding the SiNW is really helpful to reduce the intrinsic light absorption.

However, the lowest ratio of absorbed light, 5.2%, may have no practical significance as the light-concentration ability of the corresponding O-SiNW is very weak. From Fig. 2(a) it can be seen that, for an O-SiNW with a silicon core of 10 nm, the light-concentration multiples are smaller than 5.0 over all the wavelength range. And in actual, only when the core diameter becomes greater than 30 nm, a not bad light-collection performance can be obtained: the resonant peak appears and redshifts from 0.36 to 0.48 μm ; meanwhile the maximum light concentration multiple increases from 4.8 to 80.0. To characterize the full-spectrum average light-concentration ability of O-SiNWs, the *AMI.5*-weighted average extinction efficiencies, $\int_{0.3}^{0.6} Q_{ext}(\lambda)I(\lambda)d\lambda / \int_{0.3}^{0.6} I(\lambda)d\lambda$, are calculated and plotted in Fig. 2(b). Obviously, the average light concentration multiples for O-SiNWs with a core diameter smaller than 30 nm are quite small, which indicates that the light-collection ability of a single, deep-oxidized SiNW is quite bad.

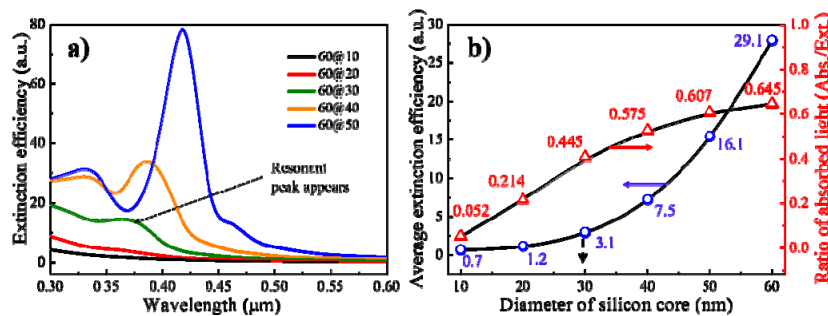


Fig. 2. Optical resonances of O-SiNWs with a constant length, 1 μm , a constant total diameter, 60 nm, but various silicon core diameters from 10 to 60 nm. (a) Extinction efficiency curves. (b) *AMI.5*-weighted ratios of the absorbed sunlight (red triangles), and average extinction efficiencies in waveband 0.3-0.6 μm (blue circles).

But the light-collection ability of a deep-oxidized SiNW array is not as awful as a single deep-oxidized SiNW, due to two reasons. The first one is that the substrate in a real system will enhance the light-collection. This is because, although the light-concentration multiples of the deep-oxidized SiNWs in Fig. 2(a) are quite small, over 65% of the leaked light by the nanowires can be absorbed by the silicon substrate again. The second reason attributes to the compactness of the O-SiNWs in a real system, as shown in Figs. 3(b)-3(d). The compact nanowires can complement each other in light-collection, thus a large light-concentration multiple becomes a nice-to-have but not a must-have feature for a single O-SiNW. These analyses can be confirmed by the fact that the measured reflectance of O-SiNW arrays [Fig. 4(a)] is only slightly greater than that of SiNW array.

Above results indicate the compactness of O-SiNWs result in a high tolerance on the light-concentration multiple of a single O-SiNW. The inverse is also true, i.e., a larger light-concentration multiple of a single O-SiNW will bring about a higher tolerance on the compactness of nanowires. In a word, for an O-SiNW array, a larger silicon core diameter means a higher compactness tolerance and a better light-trapping performance, but a greater proportion of light loss. As the O-SiNW with a core diameter of 30 nm shows obvious larger light-concentration multiple than the samples with the thinner core [Fig. 2(a)], we treat it as

the best structure in balancing the light collection multiples and the proportion of intrinsic light absorption. The percentage of absorbed light within an O-SiNW with a core diameter of 30 nm, in the whole amount of light it concentrates, is about 44.5%.

Next, the effect of oxidation on reducing the recombination ratio of the carrier before being collected is analyzed. As mentioned above, the carrier diffusion length, l , is a key parameter in calculating the recombination loss of carrier. It can be expressed as $l = \sqrt{kT/q} \times \sqrt{\mu\tau}$, where k is the Boltzmann constant, T is the temperature, q is the electron charge, μ is the carrier mobility, and τ is the carrier lifetime. It has been reported that the mobility μ of carriers in SiNW can increase from 30 to 560 cm²/V·s after passivation by forming a silica shell out it [33]. If we simply assume that τ have the same increasing multiples as μ , the carrier diffusion length in an O-SiNW can be roughly evaluated to be $560/30 \times 100 \text{ nm} \approx 1.87 \text{ }\mu\text{m}$. For the sake of conservation, we take $l = 1.5 \text{ }\mu\text{m}$ here in calculating the proportion of carrier recombination loss. The obtained value, $1 - \int_0^L 1/e^{x/l} dx = 1 - \int_0^{1000} 1/e^{x/1500} dx = 27.3\%$, is much smaller than that for a pure SiNW, 90.5%.

As a summary, taking both the amount of light being intrinsically absorbed and the recombination ratio of carriers into account, $44.5\% \times 27.3\% \approx 12.1\%$ of the concentrated sunlight by an O-SiNW will be wasted. This value is quite smaller than that in pure SiNW (58.4%), which indicates oxidation of SiNW can transport much more light into the silicon substrate.

3.3 Oxidation does not sacrifice the light-trapping ability

The effect of oxidation on reducing the proportion of intrinsic light loss in SiNW has been demonstrated above. However, only if the O-SiNW array can collect as much light as a pure SiNW array, such reduction is of practical significance. That is to say, an excellent light collection capability is the premise for a light-trapping structure. To verify the light collection performance of the O-SiNW array, we have fabricated several O-SiNW arrays with different thickness of oxide layer, and measured their reflectance spectrum curves.

Most of the reported techniques for oxidizing SiNW are developed for vapor-liquid-solid-grown SiNW [41–45] in which the residual metal particle can act as the catalyst. Therefore, these techniques are not suitable to be used to oxidize bare SiNW prepared by the metal-assisted chemical etching method. In addition, as SiNW will be wholly oxidized from top to bottom under the catalytic function of the metal particle, these techniques can't be used to fabricate O-SiNW with a silicon core. Fortunately, thermal oxidation method is specifically suitable to oxidize a bare SiNW [38–40]. And as the SiNW is gradually oxidized from the surface to the core in the thermal oxidation process, the thickness of the oxide layer can be simply controlled by oxidation time. Therefore, we chose thermal oxidation method to fabricate the O-SiNWs.

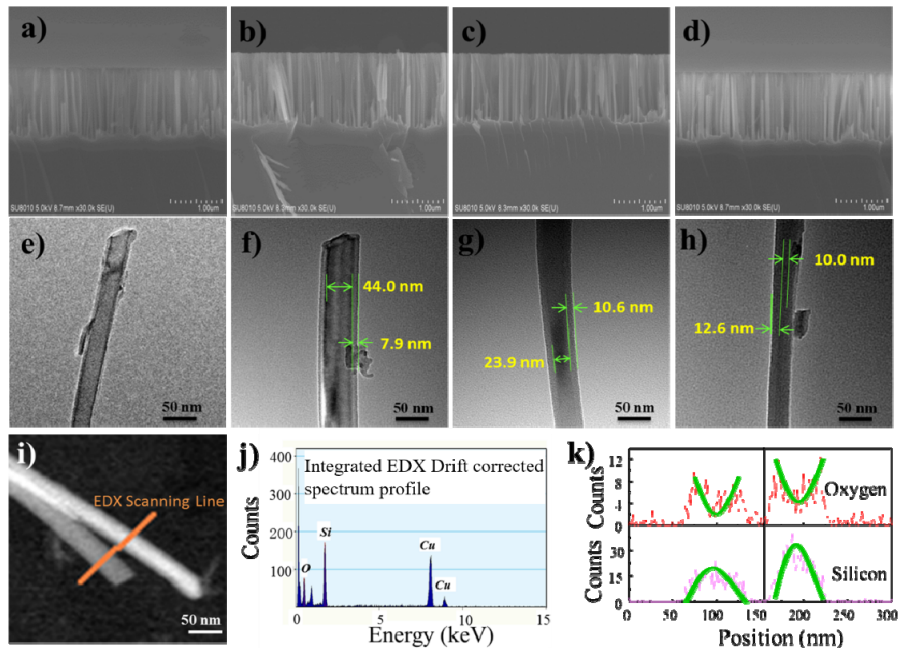


Fig. 3. Morphological features of O-SiNWs. (a-d) SEM images of SiNWs oxidized for 0, 5, 10, and 30 mins, respectively; (e-h) corresponding TEM images; (i) scanning line in the element energy-spectrum analyses for two adjacent SiNWs in the sample oxidized for 10 mins; (j) the EDX element spectrum; and (k) the EDX line profiles.

The SEM morphological characteristics of SiNWs being oxidized in a CVD tube furnace for 0, 5, 10, and 30 mins are shown in Figs. 3(a)-3(d). It can be seen that the nanowires in all the samples are compact, which is determined by the metal-assisted chemical etching technique we used. Furthermore, there is no observable difference between the morphologies of the samples. This means oxidation of SiNW should not make the nanowire thinner thus is a no-loss process. The TEM images of four single-nanowires, which corresponding to different oxidization time, are given in Figs. 3(e)-3(h). The oxide layer (silica shell) surrounding the silicon core is clearly exhibited in them, and its thickness increases gradually with the oxidation time from ~ 7.9 nm for 5 mins, to ~ 10.6 nm for 10 mins and to 12.6 nm for 30 mins. By simple calculations it can be found that the oxidation rate decreases dramatically with time, from $7.9/5 = 1.58$ nm/min to $(12.6-10.6) / (30-10) = 0.1$ nm/min. This is consistent with the previous conclusion that thermal oxidation is a self-limiting process [46].

To confirm that the observed shell in the TEM images is silica, element energy-spectrum analyses were carried out for a SiNW oxidized by 10 mins. The scanning line is marked in Fig. 3(i), which crosses over two adjacent nanowires. From the EDX element spectrum in Fig. 3(j) it can be seen that, except for the peak of the copper substrate, only the oxygen and silicon elements are detected. Besides, the line profiles of the oxygen and silicon elements in Fig. 3(k) denote a homogeneous oxide layer is formed surrounding the SiNW: they exhibit perfect upwards and downwards parabolic shape, respectively.

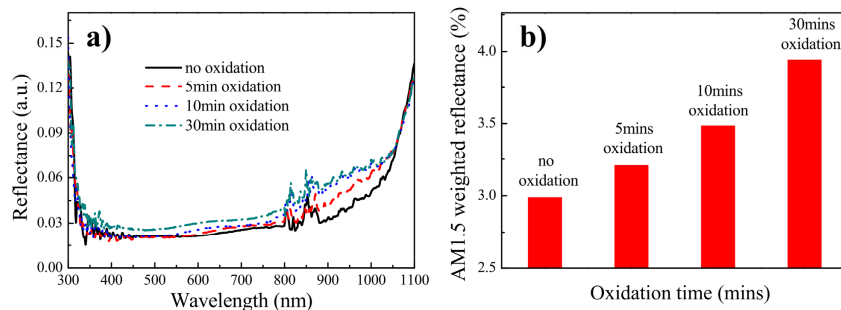


Fig. 4. Light-trapping performance of O-SiNW arrays. (a) Reflectance spectrum curves of SiNW arrays oxidized by 0, 5, 10 and 30 mins; (b) $AM1.5$ -weighted average reflectance of O-SiNW arrays.

The measured reflectance spectrum curves of SiNW arrays oxidized by 0, 5, 10 and 30 mins are shown in Fig. 4(a). It can be visually seen that the values of reflectance for O-SiNW arrays are only slightly larger than those for the pure SiNW array. To execute quantitative comparisons for the light-trapping ability of SiNW arrays oxidized by different lengths of time, the values of the $AM1.5$ -weighted average reflectance within waveband 300-1100 nm of them are calculated and plotted as a histogram in Fig. 4(b). Even for an O-SiNW array with oxidation time of 30 mins (core diameter of about 10 nm), its full-spectrum-average reflectance is only 1% greater than that of a pure SiNW array (3.9% vs. 3.0%). Therefore, oxidation almost doesn't sacrifice the anti-reflectance effect thus the light-trapping ability of SiNW array. This conclusion can be attributed to the effect of the substrate and the complementary effect of the compact nanowires as mentioned above.

Combining with the ratio of intrinsic absorption and proportion of carriers being recombined during the transport, the comprehensive sunlight loss by using a SiNW array and O-SiNW array for light-trapping can be evaluated to be $(1-3.0\%) \times 58.4\% + 3.0\% \approx 59.6\%$ and $(1-3.9\%) \times 12.1\% + 3.9\% \approx 15.5\%$, respectively. The dramatically reduced loss when using an O-SiNW array to trap sunlight is of great significance for the transformation of sunlight into electric energy with high efficiency.

3.4 Promising applications of O-SiNW

According to above analysis, O-SiNW array should be a better light-trapping structure than SiNW array. However, as it is inconvenient to directly fabricate electrode on it due to the thick silica shell, O-SiNW array must be used in specifically designed device structures. For instance, it can perform well as the light-trapping layer in all-back-contact solar cells [47] or selective-textured solar cells as shown in Fig. 5.

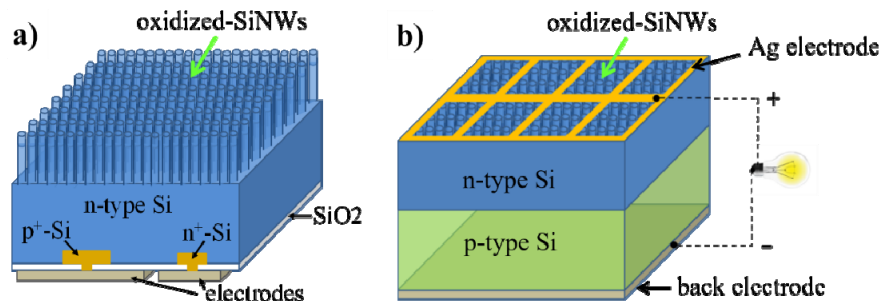


Fig. 5. Schematic illustrations of solar cells using an O-SiNW array to trap sunlight: (a) all-back-contact structure; (b) selective-textured solar cell structure.

For the all-back-contact devices, as the PN junctions are all fabricated on the back surface, it is unnecessary to fabricate electrodes on the nanowire array, thus O-SiNW array can be

directly fabricated on the front surface to trap light. The selective-textured solar cell structure in Fig. 5(b) can be fabricated by protecting the contact area from etching, which should be much simpler than the fabrication of the all-back-contact one. It has been demonstrated in the fabricating of SiNW-based solar cells that, such selective-textured structure is very helpful to improve the poor front electrode contact on the Nano-textured silicon surface (highly fluctuated), which is believed to be a big problem affecting the device performance [48,49]. According to above analysis, in both of these device structures, the sunlight harvested by O-SiNW array can be efficiently transported to the substrate; therefore, the sunlight loss should be very small.

A quantitative value of the short-circuit photocurrent density, J_{sc} , for the first architecture of solar cell in Fig. 5(a) can be estimated by the following equation,

$$J_{sc} \equiv q \cdot \left\{ (1-27.3\%) \cdot \int \frac{Q_{abs}}{Q_{ext}} \cdot F(\lambda) d\lambda + (1-3.9\%) \cdot \int \frac{1-Q_{abs}}{Q_{ext}} \cdot F(\lambda) d\lambda \right\} \cdot IQE \quad (1)$$

where, q is the electronic charge; $F(\lambda)$ is the spectral photon flux densities at air mass $AM = 1.5$; IQE is the internal quantum efficiency, whose value is simply taken as 100% here. Such estimated J_{sc} is 25.1 mA/cm². Correspondingly, if the light-trapping block is SiNWs but not O-SiNWs, the value of J_{sc} can be estimated by

$$J_{sc} \equiv q \cdot \left\{ (1-90.5\%) \cdot \int \frac{Q_{abs}}{Q_{ext}} \cdot F(\lambda) d\lambda + (1-3.0\%) \cdot \int \frac{1-Q_{abs}}{Q_{ext}} \cdot F(\lambda) d\lambda \right\} \cdot IQE. \quad (2)$$

The obtained value of J_{sc} is 19.4 mA/cm². These results indicate that using O-SiNW to replace SiNW array for light-trapping structure in the first solar cells structure can enhance the short-circuit photocurrent density by ~29%.

For the solar cells with the architecture as shown in Fig. 5(b), it is only needed to multiple a factor to taking into account the cover area of the Ag electrode. Here, we assume that the cover fraction of the Ag electrode is 5%; therefore, the values of J_{sc} using O-SiNW and SiNW array to trap sunlight are 23.8 mA/cm² and 18.4 mA/cm², respectively. The enhancement of short-circuit photocurrent density by using O-SiNW to replace SiNW array as the light-trapping block is also ~29%.

As a conclusion, using O-SiNWs as the light-trapping structure in the proposed architectures of solar cells can enhance the short-circuit photocurrent density significantly. Besides, the small light loss may be also helpful to reduce the device temperature.

4. Conclusion

In this work, we have shown that although pure SiNW has excellent light-concentration ability, a great amount of light it collects will be wasted; and we have proposed that oxidation of SiNW can significantly reduce the light loss, thus transport much more light into the silicon substrate. In pure SiNW, 64.5% of the light it collects will be absorbed within itself, and 90.5% of such absorbed light will be wasted due to the abundant carrier recombination. In a summary, 58.4% of light collected by SiNW will be wasted. Based on numerical simulations, it is found that oxidation of SiNW can significantly reduce the ratio of light being absorbed within itself, from 64.5% to 5.2%. But from another point of view, an excellent light collection capability is the premise for a light-trapping structure. Therefore, it is necessary to balance the light collection multiples of an O-SiNW and the ratio of absorbed light within itself. As a trade-off, O-SiNW with a core diameter of 30 nm was chosen as the best light-trapping structure, in which the percentage of absorbed light is 44.5%. In addition to reduce the proportion of absorbed light, oxidation can also provide good passivation for the surface of SiNW thus reduce the ratio of the recombined carrier, from 90.5% to 27.3%. Consequently, the amount of light wasted in an O-SiNW with a core diameter of 30 nm can be reduced to 12.1%, which is quite smaller than that in a pure SiNW (58.4%). To verify the

light concentration ability of O-SiNW, some O-SiNW arrays were fabricated using the thermal oxidation technique, and the thickness of the oxide layer is controlled by oxidation time. The measured reflectance spectrum curves of them demonstrate that oxidation almost doesn't sacrifice the light-trapping ability of SiNW: the *AM1.5*-weighted full-spectrum-average reflectance of the O-SiNW array is only 1% greater than that of the pure SiNW array (3.9% vs. 3.0%). In a summary, oxidation of SiNW is an easy and practical way to accomplish high-effective low-loss light-trapping. Such an O-SiNW array is promising to be used in specifically designed devices, in which the ideal short-circuit photocurrent density will be ~29% higher than using SiNW array as the light-trapping block.

Funding

National High-tech R&D Program of China (863 Program, No. 2015AA034601); National Natural Science Foundation of China (Grant Nos. 91333122, 51402106, 51372082, and 11504107); Par-Eu Scholars Program; Beijing Municipal Science and Technology Project (Z161100002616039) and the Fundamental Research Funds for the Central Universities (2016JQ01, 2015ZZD03, and 2015ZD07).